

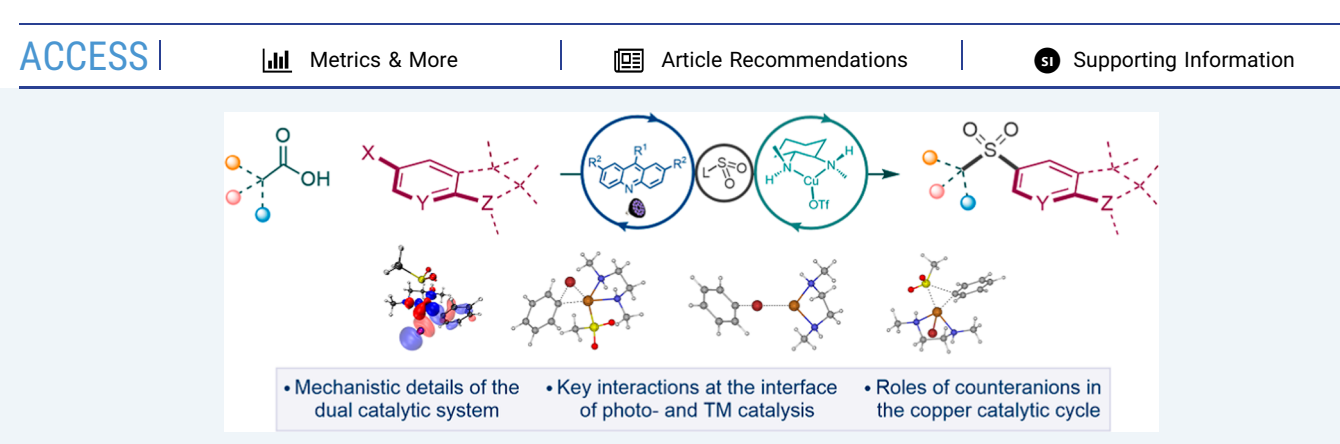
pubs.acs.org/acscatalysis Research Article

Tricomponent Decarboxysulfonylative Cross-coupling Facilitates Direct Construction of Aryl Sulfones and Reveals a Mechanistic Dualism in the Acridine/Copper Photocatalytic System

Viet D. Nguyen, Ramon Trevino, Samuel G. Greco, Hadi D. Arman, and Oleg V. Larionov*







ABSTRACT: Dual catalytic systems involving photocatalytic activation and transition metal-catalyzed steps have enabled innovative approaches to the construction of carbon—carbon and carbon—heteroatom bonds. However, the mechanistic complexity of the dual catalytic processes presents multiple challenges for understanding of the roles of divergent catalytic species that can impede the development of future synthetic methods. Here, we report a dual catalytic process that enables the previously inaccessible, broad-scope, direct conversion of carboxylic acids to aromatic sulfones—centrally important carbonyl group bioisosteric replacements and synthetic intermediates—by a tricomponent decarboxysulfonylative cross-coupling with aryl halides. Detailed mechanistic and computational studies revealed the roles of the copper catalysts, bases, and halide anions in channeling the acridine/copper system via a distinct dual catalytic manifold. In contrast to the halide-free decarboxylative conjugate addition that involves cooperative dual catalysis via low-valent copper species, the halide counteranions divert the decarboxysulfonylative cross-coupling with aryl halides through a two-phase, orthogonal relay catalytic manifold, comprising a kinetically coupled (via antithetical inhibitory and activating roles of the base in the two catalytic cycles), mechanistically discrete sequence of a photoinduced, acridine-catalyzed decarboxylative process and a thermal copper-catalyzed arylative coupling. The study underscores the importance of non-innocent roles of counteranions and key redox steps at the interface of catalytic cycles for enabling previously inaccessible dual catalytic transformations.

KEYWORDS: acridines, carboxylic acids, decarboxylation, photocatalysis, sulfones

■ INTRODUCTION

The past decade has witnessed a rapid increase in the complexity of photocatalytic systems that have evolved to combine multiple mechanistically distinct types of intertwined catalytic cycles.¹ The new photoinduced multicatalytic reactions have enabled a variety of functionalizations that harness the diverse reactivity of radical and excited state species interfaced through a variety of single-electron transfer and two-electron processes. However, the growing complexity of the emerging multicatalytic systems has posed significant challenges to mechanistic understanding of the underlying processes. In particular, the factors that determine the interactions between multiple catalytic cycles and the roles of divergent relay and cooperative multicatalytic modes remain underexplored.

Sulfones are centrally important synthetic intermediates,² pharmacophores,³ and functional linchpins in materials science applications (Scheme 1A).⁴ Their notable metabolic and physicochemical stability, as well as a distinctive chemical reactivity imparted by the sulfonyl group, have resulted in a growing number of applications that require facile and rapid synthetic access to structurally diverse sulfone-containing molecules.⁵ Given the structural and electronic similarity

Recived: May 11, 2022 Revised: June 21, 2022 Published: July 6, 2022





Scheme 1. Decarboxysulfonylative Cross-coupling of Aryl Halides and Carboxylic Acids

A. Overview of the divergent roles of alkyl aryl sulfones

B. Acridine photocatalysis: direct decarboxylative functionalizations

· Roles of divergent acridine/Cu catalytic manifolds remain unexplored

C. Tricomponent decarboxysulfonylative coupling with aryl halides

between the sulfonyl and the carbonyl groups, sulfones have emerged as efficient bioisosteric replacements for reactive carboxylic acids and other carbonyls. Notably, nearly one-half of the approved sulfone drugs feature a sulfonyl group bearing a (hetero)aryl and an alkyl substituent, underscoring the importance of the alkyl (hetero)aryl sulfones. 15

Photocatalytic direct decarboxylative functionalization has opened new directions in the synthetic methodology by enabling one-step functional group interconversions between abundant and structurally diverse carboxylic acids and other valuable functionalities without the need for preactivation of the carboxylic group. However, photoactivation of the carboxylic group toward decarboxylation poses significant challenges with respect to the scope of the acids and the diversity of carbon—carbon and carbon—heteroatom bond-forming reactions, due to the combination of the acidity of the carboxylic group that may interfere with other catalytic processes and the resistance of acids to oxidative cleavage $(E_{\rm ox} > 2.0~{\rm V}~{\rm vs}$ standard calomel electrode (SCE))¹⁰ or O—H hydrogen atom transfer (bond dissociation energy (BDE) 112 kcal/mol).¹¹

We recently described a new class of photocatalysts for visible light-induced direct decarboxylative functionalization of carboxylic acids that enabled a one-step access to several important functionalities and provided insights into the mechanistic underpinnings of complex dual and triple catalytic systems (Scheme 1B).8 The reaction scope of the new photocatalytic system has also recently been successfully expanded to the synthetically useful hydrazone additions and perfluoropyridinethiolation by the Dilman group. 9 Mechanistic studies showed that the photocatalytic decarboxylation takes place in the excited state of the acridine-carboxylic acid hydrogen bond complex without prior dissociation to acridinium carboxylate via a proton-coupled electron transfer (PCET) process. Sa,e Importantly, the acridine photocatalytic cycle could be readily interfaced with several transition metalcatalyzed (e.g., Co^{8a} and Cu^{8b-d}) processes, and the mechanisms of the catalyst turnover were specific and

Scheme 2. Mechanistic Pathways of the Dual Catalytic Decarboxysulfonylation

A.

$$RCO_2H$$
 R^2
 R^2

dependent on the mode of interactions between the acridine and the metal-catalyzed processes.

Our previous studies showed that the alkyl radical generated in the acridine photocatalytic cycle can be readily intercepted by sulfur dioxide, producing a sulfonyl radical.8d We therefore hypothesized that the sulfonyl radical can subsequently be engaged in a cross-coupling with aryl halides, resulting in net arylative decarboxysulfonylation (Scheme 1C). If developed, this method would for the first time enable a direct one-step conversion of carboxylic acids and (hetro)aryl halides that do not readily undergo nucleophilic aromatic substitution (S_NAr)¹² to aromatic sulfones. The reaction would allow for a rapid access to broad chemical space, given the ready availability and structural diversity of these two reactant classes, while by-passing preactivation and other auxiliary functional group interconversions. 13 Our earlier work on the direct decarboxylative C-S/C-N coupling reactions indicated that copper was compatible with the acridine photocatalytic cycle and facilitated the transfer of electrophiles on the sulfonyl group.8d We envisioned that the sulfonyl radical could produce sulfinic acid by a hydrogen abstraction from the acridinyl radical HA, emerging from the photoinduced PCET-enabled decarboxylation in complex B (path a, Scheme 2A). The basemediated anion exchange could then convert Cu^I complex C to sulfinate intermediate D that can undergo an oxidative addition with an aryl halide via intermediate E, followed by reductive elimination, giving rise to the sulfone product in an overall orthogonal relay dual catalytic process. 14 While the Cu^I/Cu^{III} mechanism is consistent with the roles of copper catalysis in facilitating aryl-heteroatom bond-forming reactions, 15 our mechanistic studies of the acridine/copper dual catalytic conjugate addition reactions also showed that the acridinyl radical may produce Cu⁰ species channeling the reaction via a divergent catalytic cycle within a cooperative dual catalytic system. 8c Acridinyl radical-mediated formation of Cu⁰ species could also enable an alternative mechanism for the aromatic decarboxysulfonylation that proceeds through an oxidative addition of the aryl halide to the Cu⁰ intermediate, producing arylcopper species F (path b, Scheme 2B). Subsequent crosstermination with the sulfonyl radical would lead to copper intermediate E with ensuing generation of the sulfone product by reductive elimination. Given the mechanistic dichotomy observed in the acridine/copper dual catalytic systems, further mechanistic investigation is necessary to clarify the influence of various factors that favor each pathway in order to leverage the synthetic potential of direct decarboxylation methodologies.

We report herein the development of dual catalytic acridine/ copper decarboxysulfonylation that allows for direct conversion of carboxylic acids to alkyl (hetero)aryl sulfones by a cross-coupling with aryl halides. Mechanistic studies point to key roles of halide anions in determining the operative mechanism in the copper catalytic cycle, and how it is interfaced with the acridine photocatalytic system in a twophase orthogonal relay catalytic manifold, comprising a photocatalytic decarboxylative process and a copper-catalyzed arylative cross-coupling.

RESULTS AND DISCUSSION

Optimization studies revealed that the tricomponent decarboxysulfonylative cross-coupling of carboxylic acid 1 with aryl iodide 2 occurs readily in the dual catalytic system of acridine photocatalyst A1 and diamine L1-ligated copper(I) triflate, with DABCO as a basic additive and either DABSO [DABCO.

 $(SO_2)_2$ ¹⁶ (Table 1, entry 1) or potassium metabisulfite (entry 2) as stable sulfur dioxide donors, in acetonitrile at 100 °C and

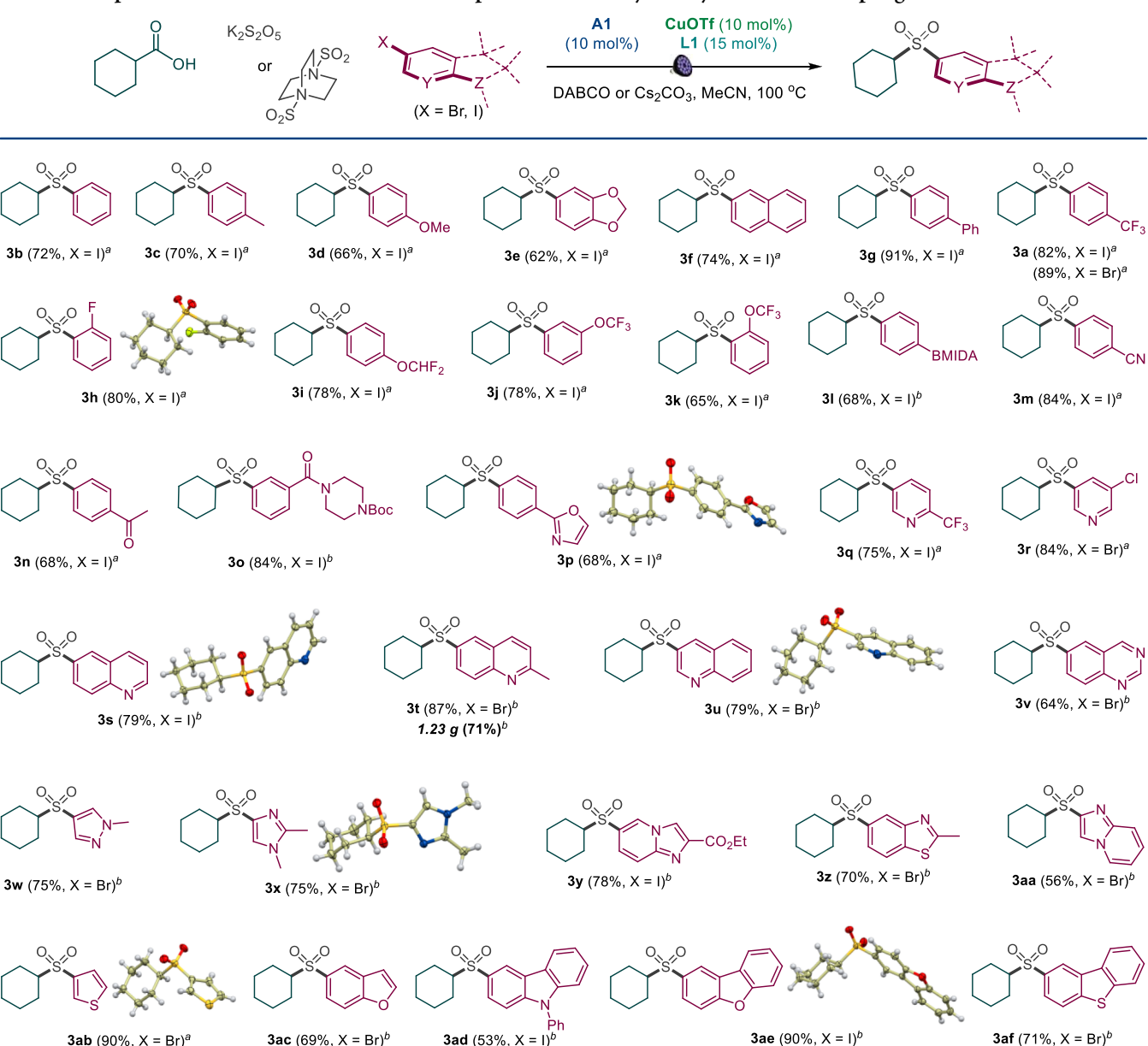
Table 1. Reaction Conditions for the Photocatalytic Direct Decarboxylative Tricomponent Coupling of Carboxylic Acids and Aryl Iodides

entry	change from optimal conditions	yield, % ^b
1	none	97 (82 ^b)
2	$K_2S_2O_5$ instead of DABSO at 100 $^{\circ}C$	91 (82 ^b)
3	no light or A1 or CuOTf	0
4	no DABCO	45
5	A2 instead of A1	73
6	A3 instead of A1	77
7	80 °C	78
8	CuBr instead of CuOTf-1/2PhMe	76
9	CuI instead of CuOTf·1/2PhMe	64
10	L2 instead of L1	41
11	L3 instead of L1	59
12	L4 instead of L1	91
13	L4 instead of L1 with $K_2S_2O_5$	88
15	PhCH ₃ instead of MeCN	19

^aReaction conditions: carboxylic acid (0.3 mmol), DABSO (0.36 mmol) or K₂S₂O₅ (0.36 mmol), aryl iodide (0.6 mmol), A1 (10 mol %), CuOTf·1/2PhMe (10 mol %), L1 (15 mol %), MeCN (3 mL), LED light (400 nm), 90 °C (for DABSO), or 100 °C (for K₂S₂O₅), 14 h. Yield was determined by ¹H NMR spectroscopy with 1,3,5trimethoxybenzene as an internal standard. ^bIsolated yield. DABSO = $O_2S-N(CH_2CH_2)_3N-SO_2$

purple LED light ($\lambda = 400 \text{ nm}$), providing sulfone 3a in 97 and 91% yields. Both catalysts and the visible light irradiation were essential for achieving the desired transformation (entry 3). DABCO was also necessary for an efficient conversion to sulfone 3a. Other acridines, for example, A2 and A3, were less suitable, while the optimal temperature was 90 °C (entries 5-7). Notably, a range of other photocatalytic systems, including N-methylacridinium salts, 4CzIPN, as well as iridium and ruthenium complexes, did not produce the sulfone product (Table S1), pointing to the key role of acridine photocatalysis in enabling the decarboxysulfonylative cross-coupling. Other copper catalyst precursors were less catalytically active (e.g., entries 8 and 9). Significant structural effects were also observed for the diamine ligand. Desmethyl ligand L2 resulted in a lower yield, indicating that a N-methyl group was necessary for the promotion of the reaction (entry 10). Interestingly, while the vicinally disubstituted diamine ligand L3 was also ineffective, the unsubstituted ligand L4 provided the product in 91% yield with DABSO and 88% with potassium metabisulfite (entries 11 and 12). Finally, acetonitrile emerged as the optimal solvent (entry 15). The acridine/copper dual-catalyzed decarboxylative conjugate addition reaction proceeded with a quantum yield of 0.06.

Table 2. Scope of Haloarenes in the Direct Tricomponent Decarboxysulfonylative Cross-coupling



"Reaction conditions for method A: carboxylic acid (0.3 mmol), $K_2S_2O_5$ (0.36 mmol), aryl iodide (0.6 mmol), A1 (10 mol %), CuOTf·1/2PhMe (10 mol %), L1 (15 mol %), DABCO (0.21 mmol), MeCN (3 mL), LED light (400 nm), 100 °C, 14 h. Breaction conditions for method B: aryl iodide (0.3 mmol), carboxylic acid (0.6 mmol), DABSO (0.72 mmol), A1 (10 mol %), CuOTf·1/2PhMe (10 mol %), L1 (15 mol %), Cs₂CO₃ (0.45 mmol), MeCN (4.5 mL), LED light (400 nm), 90 °C, 14 h. BMIDA = $B(O_2CCH_2)_2NMe$.

The scope of the aromatic coupling partners was evaluated next with carboxylic acid 1 as a substrate (Table 2). Aryl iodides bearing electron-donating alkyl and alkoxy groups were converted to sulfones 3b—3e in good yields. Sulfones 3f—3g bearing polycyclic aromatic groups were also formed in 74—91% yields. The medicinally relevant fluorine-containing groups were similarly well-tolerated (3a, 3h—3k). Notably, the reaction performed well with both aryl bromides and iodides (e.g., 3a). Other suitable coupling partners included aryl halides bearing the N-methyliminodiacetate (MIDA)-protected boryl group and cyano, keto, amide, carbamate, and 2-oxazolyl groups (3m—3p). The scope of the new sulfone synthesis can be extended to a wide array of heterocyclic halides. Nitrogenous heterocycles of the pyridine, quinoline, and quinazoline series provided the corresponding sulfone

products in good yields (3q-3v). Similarly, efficient transformations were also observed in the pyrazole, imidazole, and imidazopyridine series (3w-3y). Other heterocyclic motifs can also be readily accessed, including benzothiazole, thiophene, benzofuran, carbazole, dibenzofuran, and dibenzothiophene (3z-3af). The reaction can be performed either with the carboxylic acid (method A) or the aryl halide (method B) as a limiting reagent. While the former procedure can be carried out with potassium metabisulfite in the presence of DABCO, the latter one showed an optimal performance with DABSO and cesium carbonate.

The scope of the carboxylic acids was examined next (Table 3). Primary alkylcarboxylic acids bearing ester, ketone, carbamate, phthalimide, and thiophene groups reacted

Table 3. Scope of Carboxylic Acids in the Direct Tricomponent Decarboxysulfonylative Cross-coupling

^aMethod A. ^bMethod B. For reaction conditions, see Table 2.

smoothly and produced a range of diversely substituted sulfones 4a-4g.

The use of the deuterated methyl groups to improve the metabolic stability of drug candidates has become an established strategy in medicinal chemistry. To this end, the decarboxysulfonylation reaction can be used for a straightforward access to deuterated methyl sulfones (e.g., 4d) from the readily available d_4 -acetic acid. Sulfones 4h-4n derived from acyclic and cyclic secondary alkylcarboxylic acids, including strained and unsaturated rings (4j, 4k), were also readily produced. Notably, sulfone 4n was obtained as a single trans-diastereomer, underscoring the effect of the substrate-induced stereoselectivity. Diverse tertiary alkylcarboxylic acids were similarly well-tolerated (4o-4w), both in the acyclic and cyclic series and without any negative effects of the ring strain. Furthermore, a series of substituted adamantane-derived sulfones, including unprotected alcohol and amide-substituted

4v and 4w, were also accessed. The tricomponent decarboxysulfonylative cross-coupling can also be carried out with a range of combinations of diverse acids and arene and heteroarene coupling partners without any detriment to the reaction efficiency (4x-4ab), pointing to the applicability of the new method in a variety of structural settings.

The scope and functional group tolerance of the reaction was further examined with more structurally complex substrates, comprising natural products and active pharmaceutical ingredients (Table 4). Antihyperlipidemic gemfibrozil (5a), anti-inflammatory oxaprozin (5b), and immunosuppressive mycophenolic acid (5c) were converted to the corresponding sulfones. Similarly, the γ -sulfone analogue of glutamic acid (5d) and sulfones 5e and 5f derived from biotin and D-fructose were accessed using the new method. Bile acids were also suitable substrates (5g–5j). Likewise, halogencontaining derivatives and precursors of anxiolytic picamilon

Table 4. Arylsulfonylation of Natural Products and Pharmaceuticals by the Direct Tricomponent Decarboxysulfonylative Cross-coupling

^aMethod A. ^bMethod B. For reaction conditions, see Table 2. Aryl iodides were used unless otherwise specified.

(5k), antituberculotic bedaquiline (5l), antidiabetic empagliflozin (5m) and 5n), and canagliflozin (5o), as well as antineoplastic lapatinib (5p) all produced the desired sulfones. Furthermore, the reaction was amenable to scale-up, affording gram quantities of sulfone products (3t, 4f, and 5m). The diversity of the structural classes and functional groups in the substrates indicate that the tricomponent decarboxysulfonylative cross-coupling exhibits broad chemoselectivity that is suitable for a wide range of synthetic applications.

In order to gain insights into the thermodynamic and kinetic feasibility of the Cu^I/Cu^{III} (path a) and Cu⁰/Cu^I/Cu^{III} (path b) catalytic systems, DFT calculations were carried out. For path a, our prior studies established the thermodynamic facility of the acridine-catalyzed formation of sulfinic acids by trapping the intermediate alkyl radical with sulfur dioxide and the following hydrogen atom transfer from the intermediate acridinyl radical to the sulfonyl radical^{8d} (Scheme 2A). Building on this mechanistic analysis, attention was turned to the copper catalytic cycle (Figure 1A). The studies revealed that the halide—sulfinate anion exchange in Cu^I intermediate 6 is endergonic by 4.9 kcal/mol. Subsequent oxidative addition of aryl bromide 7 to sulfinate intermediate 8 proceeds over a

barrier of 27.6 kcal/mol (TSA) with an overall barrier of 32.5 kcal/mol from intermediate 6 that is consistent with the thermal activation required to effect the dual catalytic process.

Distortion/interaction activation strain model¹⁸ analysis points to the distortion of the aryl halide as the major contributor to the overall distortion energy in the transition state TSA (Figure 1B). Furthermore, energy decomposition analysis based on absolutely localized molecular orbitals [ALMO-EDA(solv)]¹⁹ indicates that the substantial Pauli (steric) repulsion is primarily compensated by strong electrostatic and charge transfer interactions with minor contributions from polarization and dispersion (Figure 1C). Furthermore, complementary occupied-virtual pair (COVP)²⁰ analysis shows that the most significant charge transfer takes place between the HOMO - 1 orbital of the copper complex and the LUMO + 2 of aryl halide (Figure 1D). Collectively, these results point to the key contribution of the energetic cost of breaking the strong aryl-halogen bond and the important role of the ligand in the stabilizing transition state TSA. Following the oxidative addition, the resulting intermediate 9 undergoes strong exergonic reductive elimination that is more kinetically facile than the reversal to sulfinate 8 and aryl halide, driving the

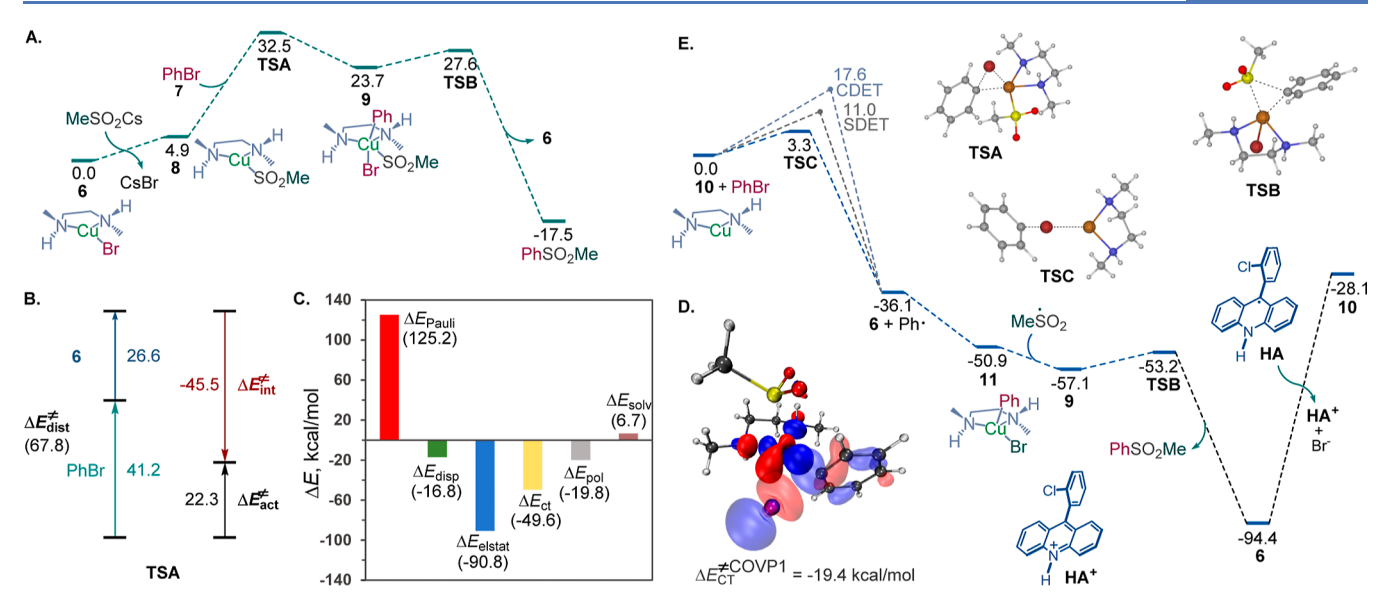


Figure 1. Computational studies of the dual catalytic decarboxysulfonylation. (A) Computed Gibbs free-energy profile for path a, ΔG , kcal/mol. (B) Activation strain model analysis for the oxidative addition to complex 8. (C) Energy decomposition analysis for TSA. (D) Most significant COVP for TSA. (E) Computed Gibbs free-energy profile for path b, ΔG , kcal/mol.

reaction forward and affording the sulfone product with concomitant regeneration of Cu^I catalyst 6. These results support the thermodynamic and kinetic feasibility of the sequential dual catalytic pathway (path a).

The acridine/Cu⁰/Cu^I/Cu^{III} catalytic pathway (path b) was examined next (Figure 1E). Given the previously established efficiency of the generation of the sulfonyl radical, 8d overall feasibility of the path b depends on the energetic parameters of the Cu-catalytic cycle and the key redox step that regenerates both the acridine and the Cu catalysts. Due to the strong reducing character of the Cu⁰ intermediate 10, the reaction with the aryl halide via a halogen atom transfer was both exergonic and readily kinetically accessible (TSC). Stepwise and concerted dissociative electron transfer pathways were also accessible but less kinetically favorable. Subsequent trapping of the aryl radical by Cu^I species 6 resulted in the exergonic formation of CuII intermediate 11, that upon an exergonic cross-termination with the sulfonyl radical, afforded intermediate 9. The ensuing reductive elimination delivered Cu¹ intermediate 6 that would need to be reduced by acridinyl radical HA to complete both catalytic cycles.

This step, however, was revealed to be highly endergonic $(\Delta G = 66.3 \text{ kcal/mol})$, pointing to a prohibitively thermodynamically unfavorable redox process that contrasted with the facility of the preceding sequence. This result is consistent with the very low reduction potentials reported for copper(I) halide complexes ($E_{\text{red}} < -2.5 \text{ V vs SCE}$),²¹ making the reduction by acridinyl radical HA ($E_{ox} = -0.66 \text{ V}$) thermodynamically unfavorable.²² These results underscore the importance of the redox steps at the intersection of the catalytic cycles 1a,b,8c and highlight the differences in the redox properties of the more readily reducible cationic Cu^I/Cu⁰ systems with labile counteranions (e.g., tetrafluoroborate) and the substantially more stable copper(I) halide systems that may lead to distinctive mechanistic behavior in dual catalytic reactions. Comparing the mechanisms of the direct decarboxylative conjugate addition catalyzed by a cationic Cu^I complex with a labile tetrafluoroborate anion8c with path b of the arylative decarboxysulfonylation, it is evident that the halide

plays a key role in diverting the reaction from path b by forestalling the key catalyst turnover redox step in the otherwise kinetically and thermodynamically favorable pathway.

To gain experimental support for the computationally derived pathway, mechanistic and kinetic studies were carried out for the decarboxysulfonylative coupling and the individual catalytic cycles (i.e., the acridine-catalyzed sulfinic acid formation and the copper-catalyzed cross-coupling). Addition of TEMPO led to the suppression of the decarboxysulfonylation and formation of the alkyl radical trapping product 12, indicating that the reaction involves the decarboxylation-derived alkyl radical (Figure 2A). In contrast, no aryl-TEMPO 13 product was observed. Similarly, a reaction with aryl iodide 14 produced sulfone 15 without cyclization that involves the pendant allyl group (i.e., formation of sulfone 16, Figure 2B). These results suggest that the aryl radical is not involved in the sulfonylation step, pointing to the oxidative addition as the C–X bond activation pathway.

Interestingly, the acridine-catalyzed sulfinic acid production rate was 2.8 times higher than the overall rate of the sulfone production in the decarboxysulfonylative dual catalytic system (Figure 2C,D, no DABCO). Despite the substantially faster sulfinic acid production, no accumulation of the sulfinic acid was observed in the initial stages of the decarboxysulfonylative process in the presence of DABCO (Figure 2D, with DABCO).

Further studies revealed that the Cu-catalyzed cross-coupling of intermediate sulfinate salt 17 with the aryl halide proceeded at the same rate as decarboxysulfonylation (Figure 2D,E). These results suggest that the overall rate of decarboxysulfonylation is controlled by the Cu-catalyzed sulfinate—aryl halide cross-coupling, while the rate of the acridine-catalyzed sulfinic acid production is dampened under the optimal decarboxysulfonylation conditions to be better aligned with the Cu-catalyzed process. This observation is supported by the accumulation of the sulfinate in the dual catalytic process in the absence of DABCO in contrast to the DABCO-mediated reaction (Figure 2D). We hypothesized

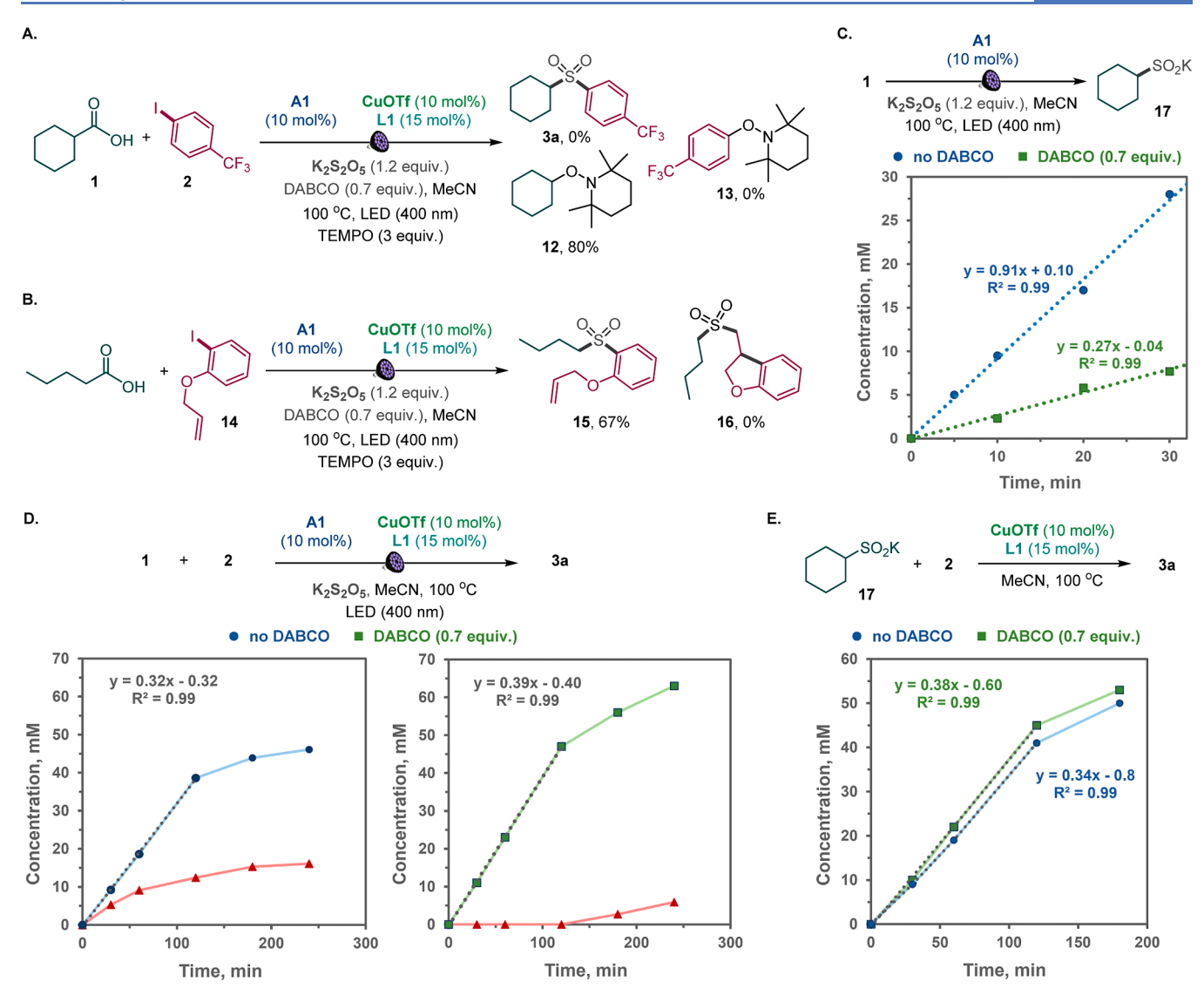


Figure 2. Kinetic profile of dual catalytic decarboxysulfonylation. (A) Radical trapping experiment with TEMPO. (B) Cyclization experiment with aryl iodide 14. (C) Kinetics of the photoinduced decarboxylative sulfination of acid 1 at 100 °C with (green squares) and without (blue dots) added DABCO. (D) Kinetics of the decarboxysulfonylation (blue dots) and the accumulation of sulfinate salt 17 (red triangles) during the decarboxysulfonylation. (E) Kinetic profile of the cross-coupling of sulfinate 17 and aryl iodide 2. The experiments were carried out under the method A reaction conditions with or without irradiation, as specified in each reaction scheme.

that DABCO may play a dual role of the promoter of the Cucatalyzed step (Figure 2E) as a basic proton shuttle (i.e., B in Scheme 2A) and an inhibitor of the acridine-catalyzed step. This result was expected to be in line with our previous studies that demonstrated the inhibitory effect of added amine bases on the acridine-catalyzed decarboxylative reactions. 8a-c Indeed, when the acridine-catalyzed sulfinic acid formation was carried out in the presence of DABCO to match the decarboxysulfonylation conditions, the reaction rate decreased and was close to the rate of decarboxysulfonylation (Figure 2C). The identical rates of the Cu-catalyzed sulfinate-aryl halide coupling in the presence of a stoichiometric amount of the sulfinate and the decarboxysulfonylation proceeding with low free sulfinate concentrations also suggested that the Cucatalyzed coupling was of zero order in the sulfinate. Kinetic studies based on the variable time normalization analysis²⁴ and the initial rate method revealed that the Cu-catalyzed sulfinate-aryl halide coupling was indeed of zero order in the sulfinate, as well as DABCO, and of first order in both the

Cu catalyst and the aryl halide (Figure 3). This result is congruent with the oxidative addition as the rate-limiting step, in line with the computationally derived path a mechanism. Taken together, the computational and experimental studies indicate that the decarboxysulfonylative cross-coupling of carboxylic acids with aryl halides proceeds by an orthogonal relay dual catalytic process, comprising a photocatalytic formation of the sulfinate intermediate in the acridine photocatalytic cycle and a copper-catalyzed cross-coupling of the sulfinate intermediate with aryl halide channeled via path a, that is through an oxidative addition of aryl halide to a copper(I) sulfinate complex with subsequent reductive elimination en route to the aryl sulfone product.

CONCLUSIONS

In summary, we have developed a visible light-induced, dual catalytic, direct decarboxysulfonylative cross-coupling of carboxylic acids with aryl halides. The reaction enables the previously inaccessible construction of alkyl aryl sulfones

ACS Catalysis pubs.acs.org/acscatalysis Research Article

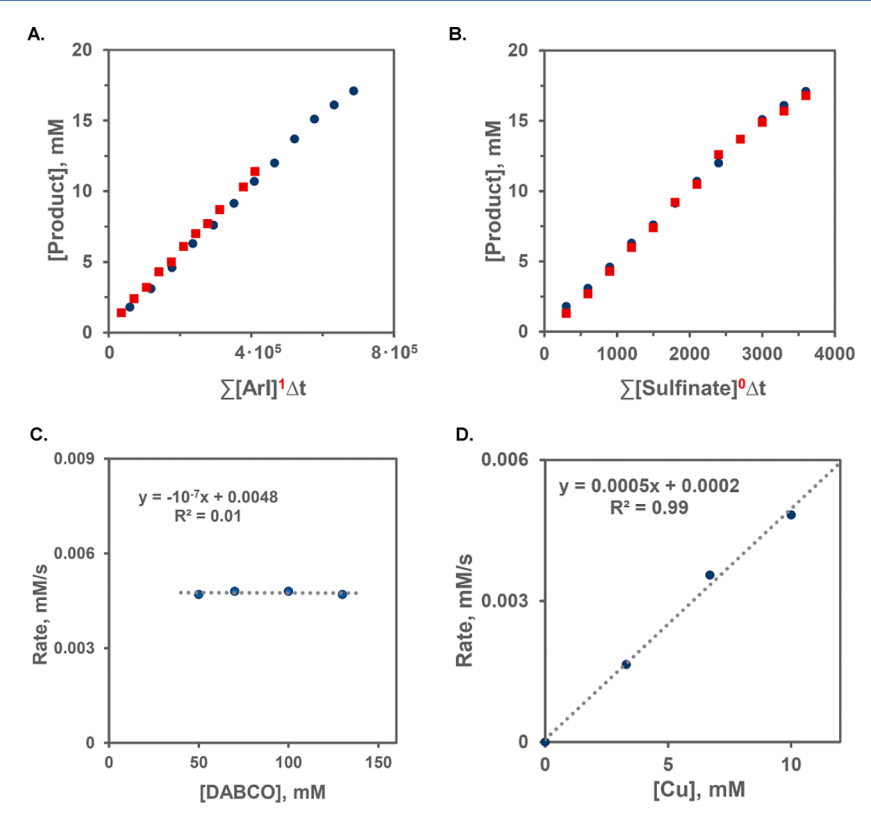


Figure 3. Kinetic studies of the copper-catalyzed cross-coupling of aryl iodide 2 and sulfinate 17. (A) Order in aryl iodide 2. (B) Order in sulfinate 17. (C) Order in DABCO. (D) Order in the copper catalyst. The experiments were carried out according to method A in the absence of the acciding photocatalyst and without irradiation.

directly from carboxylic acids without preactivation and has a broad scope with respect to the acid and aryl halide coupling partners, providing a route for the direct interconversion of the bioisosteric carboxylic and sulfonyl groups. Mechanistic and computational studies revealed that the acridine/copper dual catalytic system facilitates the tricomponent decarboxysulfonylative coupling by an orthogonal relay catalytic pathway that is distinct from the previously described decarboxylative conjugate addition system, underscoring the import roles of halide anions in channeling the dual catalytic system via a divergent process that comprises acridine-catalyzed decarboxylative generation of an alkyl radical followed by the formation of an alkylsulfinate intermediate and the ensuing coppercatalyzed sulfinate cross-coupling with aryl halides. The studies highlight the mechanistic versatility of the acridine/copper dual catalytic system and point to new opportunities in catalytic carbon-heteroatom bond formation.

ASSOCIATED CONTENT

Supporting Information

The Supporting Information is available free of charge at https://pubs.acs.org/doi/10.1021/acscatal.2c02332.

Experimental and spectral details for all new compounds and all reactions reported (PDF)

X-ray crystallographic details (ZIP)

AUTHOR INFORMATION

Corresponding Author

Oleg V. Larionov – Department of Chemistry, The University of Texas at San Antonio, San Antonio, Texas 78249, United

States; o orcid.org/0000-0002-3026-1135; Email: oleg.larionov@utsa.edu

Authors

Viet D. Nguyen – Department of Chemistry, The University of Texas at San Antonio, San Antonio, Texas 78249, United States

Ramon Trevino – Department of Chemistry, The University of Texas at San Antonio, San Antonio, Texas 78249, United States

Samuel G. Greco – Department of Chemistry, The University of Texas at San Antonio, San Antonio, Texas 78249, United States

Hadi D. Arman – Department of Chemistry, The University of Texas at San Antonio, San Antonio, Texas 78249, United

Complete contact information is available at: https://pubs.acs.org/10.1021/acscatal.2c02332

Notes

The authors declare no competing financial interest.

ACKNOWLEDGMENTS

Financial support by the NIGMS (GM134371) and NSF (CHE-2102646) is gratefully acknowledged. The UTSA NMR and X-ray crystallography facilities were supported by the NSF (CHE-1625963 and CHE-1920057). The authors acknowledge the Texas Advanced Computing Center (TACC) and the Extreme Science and Engineering Discovery Environment (XSEDE) for providing computational resources.

REFERENCES

(1) (a) Chan, A. Y.; Perry, I. B.; Bissonnette, N. B.; Buksh, B. F.; Edwards, G. A.; Frye, L. I.; Garry, O. L.; Lavagnino, M. N.; Li, B. X.; Liang, Y.; Mao, E.; Millet, A.; Oakley, J. V.; Reed, N. L.; Sakai, H. A.; Seath, C. P.; MacMillan, D. W. C. Metallaphotoredox: The Merger of Photoredox and Transition Metal Catalysis. *Chem. Rev.* 2022, 122, 1485–1542. (b) Skubi, K. L.; Blum, T. R.; Yoon, T. P. Dual Catalysis Strategies in Photochemical Synthesis. *Chem. Rev.* 2016, 116, 10035–10074. (c) Hossain, A.; Bhattacharyya, A.; Reiser, O. Copper's rapid ascent in visible-light photoredox catalysis. *Science* 2019, 364, No. eaav9713. (d) Cheng, W.-M.; Shang, R. Transition Metal-Catalyzed Organic Reactions under Visible Light: Recent Developments and Future Perspectives. *ACS Catal.* 2020, 10, 9170–9196. (e) Cheung, K. P. S.; Sarkar, S.; Gevorgyan, V. Visible Light-Induced Transition Metal Catalysis. *Chem. Rev.* 2022, 122, 1543–1625.

(2) (a) Patai, S. The Chemistry of Sulfinic Acids, Esters and Their Derivatives; John Wiley & Sons, Ltd: New Jersey, 1990. (b) Patai, S.; Rapport, Z. The Chemistry of Sulfonic Acids, Esters and Their Derivatives; John Wiley & Sons: New York, 1991. (c) Aïssa, C. Mechanistic Manifold and New Developments of the Julia-Kocienski Reaction. Eur. J. Org. Chem. 2009, 2009, 1831-1844. (d) García-Domínguez, A.; Müller, S.; Nevado, C. Nickel-Catalyzed Intermolecular Carbosulfonylation of Alkynes via Sulfonyl Radicals. Angew. Chem., Int. Ed. 2017, 56, 9949-9952. (e) Burke, E. G.; Gold, B.; Hoang, T. T.; Raines, R. T.; Schomaker, J. M. Fine-Tuning Strain and Electronic Activation of Strain-Promoted 1,3-Dipolar Cycloadditions with Endocyclic Sulfamates in SNO-OCTs. J. Am. Chem. Soc. 2017, 139, 8029-8037. (f) Nguyen, V. T.; Dang, H. T.; Pham, H. H.; Nguyen, V. D.; Flores-Hansen, C.; Arman, H. D.; Larionov, O. V. Highly Regio-and Stereoselective Catalytic Synthesis of Conjugated Dienes and Polyenes. J. Am. Chem. Soc. 2018, 140, 8434-8438. (g) Ratushnyy, M.; Kamenova, M.; Gevorgyan, V. A Mild Light-Induced Cleavage of the S-O Bond of Aryl Sulfonate Esters Enables Efficient Sulfonylation of Vinylarenes. Chem. Sci. 2018, 9, 7193-7197. (h) Ariki, Z. T.; Maekawa, Y.; Nambo, M.; Crudden, C. M. Preparation of Quaternary Centers via Nickel-Catalyzed Suzuki-Miyaura Cross-Coupling of Tertiary Sulfones. J. Am. Chem. Soc. 2018, 140, 78-81. (i) Nambo, M.; Yim, J. C.-H.; Freitas, L. B. O.; Tahara, Y.; Ariki, Z. T.; Maekawa, Y.; Yokogawa, D.; Crudden, C. M. Modular Synthesis of α -Fluorinated Arylmethanes via Desulfonative Cross-Coupling. Nat. Commun. 2019, 10, 4528. (j) Hell, S. M.; Meyer, C. F.; Misale, A.; Sap, J. B. I.; Christensen, K. E.; Willis, M. C.; Trabanco, A. A.; Gouverneur, V. Hydrosulfonylation of Alkenes with Sulfonyl Chlorides under Visible Light Activation. Angew. Chem., Int. Ed. 2020, 59, 11620-11626. (k) Chu, X.-Q.; Ge, D.; Cui, Y.-Y.; Shen, Z.-L.; Li, C.-J. Desulfonylation via Radical Process: Recent Developments in Organic Synthesis. Chem. Rev. 2021, 121, 12548-12680. (1) Nambo, M.; Maekawa, Y.; Crudden, C. M. Desulfonylative Transformations of Sulfones by Transition-Metal Catalysis, Photocatalysis, and Organocatalysis. ACS Catal. 2022, 12, 3013-3032.

- (3) (a) Ilardi, E. A.; Vitaku, E.; Njardarson, J. T. Data-Mining for Sulfur and Fluorine: An Evaluation of Pharmaceuticals To Reveal Opportunities for Drug Design and Discovery. *J. Med. Chem.* **2014**, 57, 2832–2842. (b) Scott, K. A.; Njardarson, J. T. Analysis of US FDA-Approved Drugs Containing Sulfur Atoms. *Top. Curr. Chem.* **2018**, 376, 5.
- (4) (a) Kausar, A.; Zulfiqar, S.; Sarwar, M. I. Recent Developments in Sulfur-Containing Polymers. *Polym. Rev.* **2014**, *54*, 185–267. (b) Bell, W. K.; Rawlings, B. M.; Long, B. K.; Webb, R. C.; Keitz, B. K.; Häußling, L.; Willson, C. G. Poling and crosslinking processes in NLO polymers. *J. Polym. Sci., Part A: Polym. Chem.* **2014**, *52*, 2769–2775.
- (5) For recent approaches to sulfones, see: (a) Emmett, E. J.; Hayter, B. R.; Willis, M. C. Palladium-Catalyzed Synthesis of Ammonium Sulfinates from Aryl Halides and a Sulfur Dioxide Surrogate: A Gas-and Reductant-Free Process. *Angew. Chem., Int. Ed.* **2014**, *53*, 10204–10208. (b) Deeming, A. S.; Russell, C. J.; Hennessy, A. J.; Willis, M. C. DABSO-Based, Three-Component, One-Pot Sulfone Synthesis. *Org. Lett.* **2014**, *16*, 150–153. (c) Johnson, M. W.;

Bagley, S. W.; Mankad, N. P.; Bergman, R. G.; Mascitti, V.; Toste, F. D. Application of Fundamental Organometallic Chemistry to the Development of a Gold-Catalyzed Synthesis of Sulfinate Derivatives. Angew. Chem., Int. Ed. 2014, 53, 4404-4407. (d) Shavnya, A.; Coffey, S. B.; Smith, A. C.; Mascitti, V. Palladium-Catalyzed Sulfination of Aryl and Heteroaryl Halides: Direct Access to Sulfones and Sulfonamides. Org. Lett. 2013, 15, 6226-6229. (e) Margraf, N.; Manolikakes, G. One-Pot Synthesis of Aryl Sulfones from Organometallic Reagents and Iodonium Salts. J. Org. Chem. 2015, 80, 2582-2600. (f) Shavnya, A.; Hesp, K. D.; Mascitti, V.; Smith, A. C. Palladium-Catalyzed Synthesis of (Hetero) Aryl Alkyl Sulfones from (Hetero) Aryl Boronic Acids, Unactivated Alkyl Halides, and Potassium Metabisulfite. Angew. Chem., Int. Ed. 2015, 54, 13571-13575. (g) Chen, Y.; Willis, M. C. Copper (I)-Catalyzed Sulfonylative Suzuki-Miyaura Cross-Coupling. Chem. Sci. 2017, 8, 3249-3253. (h) Gong, X.; Ding, Y.; Fan, X.; Wu, J. Synthesis of β -Keto Sulfones via Coupling of Aryl/Alkyl Halides, Sulfur Dioxide and Silyl Enolates through Metal-Free Photoinduced C-X Bond Dissociation. Adv. Synth. Catal. 2017, 359, 2999-3004. (i) Griffiths, R. J.; Kong, W. C.; Richards, S. A.; Burley, G. A.; Willis, M. C.; Talbot, E. P. A. Oxidative β-C-H Sulfonylation of Cyclic Amines. Chem. Sci. 2018, 9, 2295-2300. (j) He, J.; Chen, G.; Zhang, B.; Li, Y.; Chen, J.-R.; Xiao, W.-J.; Liu, F.; Li, C. Catalytic Decarboxylative Radical Sulfonylation. Chem 2020, 6, 1149-1159. (k) Li, Y.; Chen, S.; Wang, M.; Jiang, X. Sodium Dithionite-Mediated Decarboxylative Sulfonylation: Facile Access to Tertiary Sulfones. Angew. Chem., Int. Ed. 2020, 59, 8907-8911. (1) Jin, S.; Haug, G. C.; Trevino, R.; Nguyen, V. D.; Arman, H. D.; Larionov, O. V. Photoinduced C(sp3)-H Sulfination Empowers a Direct and Chemoselective Introduction of the Sulfonyl Group. Chem. Sci. 2021, 12, 13914-13921. (m) Sarver, P. J.; Bissonnette, N. B.; MacMillan, D. W. C. Decatungstate-Catalyzed C(sp3)-H Sulfinylation: Rapid Access to Diverse Organosulfur Functionality. J. Am. Chem. Soc. 2021, 143, 9737-9743. (n) Granados, A.; Cabrera-Afonso, M. J.; Escolano, M.; Badir, S. O.; Molander, G. A. Thianthreniumenabled sulfonylation via electron donor-acceptor complex photoactivation. Chem. Catal. 2022, 2, 898-907.

- (6) (a) Patani, G. A.; LaVoie, E. J. Bioisosterism: A Rational Approach in Drug Design. *Chem. Rev.* **1996**, 96, 3147–3176. (b) Smith, D. A. *Metabolism, Pharmacokinetics and Toxicity of Functional Groups*; Royal Society of Chemistry: London, United Kingdom, 2010; pp 99–167.
- (7) (a) Kautzky, J. A.; Wang, T.; Evans, R. W.; MacMillan, D. W. C. Decarboxylative Trifluoromethylation of Aliphatic Carboxylic Acids. J. Am. Chem. Soc. 2018, 140, 6522-6526. (b) Till, N. A.; Smith, R. T.; MacMillan, D. W. C. Decarboxylative Hydroalkylation of Alkynes. J. Am. Chem. Soc. 2018, 140, 5701-5705. (c) Sun, X.; Chen, J.; Ritter, T. Catalytic Dehydrogenative Decarboxyolefination of Carboxylic Acids. Nat. Chem. 2018, 10, 1229-1233. (d) Cartwright, K. C.; Tunge, J. A. Decarboxylative Elimination of N-Acyl Amino Acids via Photoredox/Cobalt Dual Catalysis. ACS Catal. 2018, 8, 11801-11806. (e) Cartwright, K. C.; Lang, S. B.; Tunge, J. A. Photoinduced Kochi Decarboxylative Elimination for the Synthesis of Enamides and Enecarbamates from N-Acyl Amino Acids. J. Org. Chem. 2019, 84, 2933-2940. (f) Faraggi, T. M.; Li, W.; MacMillan, D. W. C. Decarboxylative Oxygenation via Photoredox Catalysis. Isr. J. Chem. 2020, 60, 410-415. (g) Li, J.; Huang, C.-Y.; Han, J.-T.; Li, C.-J. Development of a Quinolinium/Cobaloxime Dual Photocatalytic System for Oxidative C-C Cross-Couplings via H2 Release. ACS Catal. 2021, 11, 14148-14158. (h) Li, Q. Y.; Gockel, S. N.; Lutovsky, G. A.; DeGlopper, K. S.; Baldwin, N. J.; Bundesmann, M. W.; Tucker, J. W.; Bagley, S. W.; Yoon, T. P. Decarboxylative Cross-Nucleophile Coupling via Ligand-to-Metal Charge Transfer Photoexcitation of Cu(II) Carboxylates. Nat. Chem. 2022, 14, 94-99. For a review, see: (i) Shang, R.; Liu, L. Transition metal-catalyzed decarboxylative cross-coupling reactions. Sci. China: Chem. 2011, 54, 1670-1687. (j) Kitcatt, D. M.; Nicolle, S.; Lee, A.-L. Direct Decarboxylative Giese Reactions. Chem. Soc. Rev. 2022, 51, 1415-1453.
- (8) (a) Nguyen, V. T.; Nguyen, V. D.; Haug, G. C.; Dang, H. T.; Jin, S.; Li, Z.; Flores-Hansen, C.; Benavides, B. S.; Arman, H. D.;

Larionov, O. V. Alkene Synthesis by Photocatalytic, Chemoenzymatically-Compatible Dehydrodecarboxylation of Carboxylic Acids and Biomass. ACS Catal. 2019, 9, 9485-9498. (b) Nguyen, V. T.; Nguyen, V. D.; Haug, G. C.; Vuong, N. T. H.; Dang, H. T.; Arman, H. D.; Larionov, O. V. Visible-Light-Enabled Direct Decarboxylative N-Alkylation. Angew. Chem., Int. Ed. 2020, 59, 7921-7927. (c) Dang, H. T.; Haug, G. C.; Nguyen, V. T.; Vuong, N. T. H.; Nguyen, V. D.; Arman, H. D.; Larionov, O. V. Acridine Photocatalysis: Insights into the Mechanism and Development of a Dual Catalytic Direct Decarboxylative Conjugate Addition. ACS Catal. 2020, 10, 11448-11457. (d) Nguyen, V. T.; Haug, G. C.; Nguyen, V. D.; Vuong, N. T. H.; Arman, H. D.; Larionov, O. V. Photocatalytic Decarboxylative Amidosulfonation Enables Direct Transformation of Carboxylic Acids to Sulfonamides. Chem. Sci. 2021, 12, 6429-6436. (e) Nguyen, V. T.; Haug, G. C.; Nguyen, V. D.; Vuong, N. T. H.; Karki, G. B.; Arman, H. D.; Larionov, O. V. Functional Group Divergence and the Structural Basis of Acridine Photocatalysis Revealed by Direct Decarboxysulfonylation. Chem. Sci. 2022, 13, 4170-4179.

- (9) (a) Dmitriev, I. A.; Levin, V. V.; Dilman, A. D. Boron Chelates Derived from N-Acylhydrazones as Radical Acceptors: Photocatalyzed Coupling of Hydrazones with Carboxylic Acids. Org. Lett. 2021, 23, 8973—8977. (b) Zubkov, M. O.; Kosobokov, M. D.; Levin, V. V.; Dilman, A. D. Photocatalyzed Decarboxylative Thiolation of Carboxylic Acids Enabled by Fluorinated Disulfide. Org. Lett. 2022, 24, 2354—2358. See also: (c) Zubkov, M. O.; Kosobokov, M. D.; Levin, V. V.; Kokorekin, V. A.; Korlyukov, A. A.; Hu, J.; Dilman, A. D. A novel photoredox-active group for the generation of fluorinated radicals from difluorostyrenes. Chem. Sci. 2020, 11, 737—741.
- (10) Sawyer, D. T.; Sobkowiak, A.; Roberts, J. L. Electrochemistry for Chemists, 2nd ed.; Wiley: New York, 1995; p 125.
- (11) Blanksby, S. J.; Ellison, G. B. Bond Dissociation Energies of Organic Molecules. *Acc. Chem. Res.* **2003**, *36*, 255–263.
- (12) Nguyen, V. D.; Nguyen, V. T.; Haug, G. C.; Dang, H. T.; Arman, H. D.; Ermler, W. C.; Larionov, O. V. Rapid and Chemodivergent Synthesis of N-Heterocyclic Sulfones and Sulfides: Mechanistic and Computational Details of the Persulfate-Initiated Catalysis. ACS Catal. 2019, 9, 4015–4024.
- (13) Crossley, S. W. M.; Shenvi, R. A. A Longitudinal Study of Alkaloid Synthesis Reveals Functional Group Interconversions as Bad Actors. *Chem. Rev.* **2015**, *115*, 9465–9531.
- (14) Inamdar, S. M.; Shinde, V. S.; Patil, N. T. Enantioselective Cooperative Catalysis. *Org. Biomol. Chem.* **2015**, *13*, 8116–8162.
- (15) (a) Ma, D.; Cai, Q. Copper/Amino Acid Catalyzed Cross-Couplings of Aryl and Vinyl Halides with Nucleophiles. Acc. Chem. Res. 2008, 41, 1450-1460. (b) Jones, G. O.; Liu, P.; Houk, K. N.; Buchwald, S. L. Computational Explorations of Mechanisms and Ligand-Directed Selectivities of Copper-Catalyzed Ullmann-Type Reactions. J. Am. Chem. Soc. 2010, 132, 6205-6213. (c) Amal Joseph, P. J.; Priyadarshini, S. Copper-Mediated C-X Functionalization of Aryl Halides. Org. Process Res. Dev. 2017, 21, 1889-1924. (d) Bhunia, S.; Pawar, G. G.; Kumar, S. V.; Jiang, Y.; Ma, D. Selected copper-based reactions for C-N, C-O, C-S, and C-C bond formation. Angew. Chem., Int. Ed. 2017, 56, 16136-16179. (e) Chen, Z.; Jiang, Y.; Zhang, L.; Guo, Y.; Ma, D. Oxalic Diamides and tert-Butoxide: Two Types of Ligands Enabling Practical Access to Alkyl Aryl Ethers via Cu-Catalyzed Coupling Reaction. J. Am. Chem. Soc. 2019, 141, 3541-3549. See also: (f) Cabrera-Afonso, M. J.; Lu, Z.-P.; Kelly, C. B.; Lang, S. B.; Dykstra, R.; Gutierrez, O.; Molander, G. A. Engaging sulfinate salts via Ni/photoredox dual catalysis enables facile Csp²-SO₂R coupling. Chem. Sci. 2018, 9, 3186-3191.
- (16) Woolven, H.; González-Rodríguez, C.; Marco, I.; Thompson, A. L.; Willis, M. C. DABCO-Bis(Sulfur Dioxide), DABSO, as a Convenient Source of Sulfur Dioxide for Organic Synthesis: Utility in Sulfonamide and Sulfamide Preparation. *Org. Lett.* **2011**, *13*, 4876–4878.
- (17) (a) Gant, T. G. Using deuterium in drug discovery: leaving the label in the drug. *J. Med. Chem.* **2014**, *57*, 3595–3611. (b) Pirali, T.; Serafini, M.; Cargnin, S.; Genazzani, A. A. Applications of Deuterium in Medicinal Chemistry. *J. Med. Chem.* **2019**, *62*, 5276–5297.

- (18) Bickelhaupt, F. M.; Houk, K. N. Analyzing Reaction Rates with the Distortion/Interaction-Activation Strain Model. *Angew. Chem., Int. Ed.* **2017**, *56*, 10070–10086.
- (19) (a) Horn, P. R.; Sundstrom, E. J.; Baker, T. A.; Head-Gordon, M. Unrestricted Absolutely Localized Molecular Orbitals for Energy Decomposition Analysis: Theory and Applications to Intermolecular Interactions Involving Radicals. J. Chem. Phys. 2013, 138, 134119—134132. (b) Horn, P. R.; Mao, Y.; Head-Gordon, M. Probing Non-Covalent Interactions with a Second-Generation Energy Decomposition Analysis Using Absolutely Localized Molecular Orbitals. Phys. Chem. Chem. Phys. 2016, 18, 23067—23079.
- (20) Khaliullin, R. Z.; Bell, A. T.; Head-Gordon, M. Analysis of Charge Transfer Effects in Molecular Complexes Based on Absolutely Localized Molecular Orbitals. *J. Chem. Phys.* **2008**, *128*, 184112.
- (21) Romanov, A. S.; Becker, C. R.; James, C. E.; Di, D.; Credgington, D.; Linnolahti, M.; Bochmann, M. Copper and Gold Cyclic (Alkyl)(amino)carbene Complexes with Sub-Microsecond Photoemissions: Structure and Substituent Effects on Redox and Luminescent Properties. *Chem.—Eur. J.* 2017, 23, 4625–4637.
- (22) The redox step was also highly kinetically unfavorable, with the barriers to the concerted and stepwise electron transfers of 74.8 and 95.7 kcal/mol.
- (23) For examples of trapping aryl radicals with TEMPO, see: (a) Iwata, Y.; Tanaka, Y.; Kubosaki, S.; Morita, T.; Yoshimi, Y. A strategy for generating aryl radicals from arylborates through organic photoredox catalysis: photo-Meerwein type arylation of electron-deficient alkenes. *Chem. Commun.* **2018**, *54*, 1257–1260. (b) Xu, Z.-J.; Liu, X.-Y.; Zhu, M.-Z.; Xu, Y.-L.; Yu, Y.; Xu, H.-R.; Cheng, A.-X.; Lou, H.-X. Photoredox-Catalyzed Cascade Reactions Involving Aryl Radical: Total Synthesis of (±)-Norascyronone A and (±)-Eudesmol. *Org. Lett.* **2021**, *23*, 9073–9077.
- (24) Burés, J. Variable Time Normalization Analysis: General Graphical Elucidation of Reaction Orders from Concentration Profiles. *Angew. Chem., Int. Ed.* **2016**, *55*, 16084–16087.

□ Recommended by ACS

Copper-Catalyzed Intermolecular Functionalization of Unactivated C(sp3)-H Bonds and Aliphatic Carboxylic Acids

Runze Mao, Xile Hu, et al.

AUGUST 31, 2021

JOURNAL OF THE AMERICAN CHEMICAL SOCIETY

READ 🗹

Visible Light-Induced Transition Metal Catalysis

Kelvin Pak Shing Cheung, Vladimir Gevorgyan, et al.

OCTOBER 08, 2021

CHEMICAL REVIEWS

READ 🗹

Selective Difunctionalization of Unactivated Aliphatic Alkenes Enabled by a Metal-Metallaaromatic Catalytic System

Fei-Hu Cui, Haiping Xia, et al.

JANUARY 25, 2022

JOURNAL OF THE AMERICAN CHEMICAL SOCIETY

READ [7

Dual Ligand Enabled Nondirected C-H Chalcogenation of Arenes and Heteroarenes

Soumya Kumar Sinha, Debabrata Maiti, et al.

JUNE 27, 2022

JOURNAL OF THE AMERICAN CHEMICAL SOCIETY

READ 🗹

Get More Suggestions >